Supporting Information:

Apart from the attenuation of the nickel signals as shown in Figure 1 and Figure S1a, additional information on the growth behaviour of [C_1C_1Im][Tf_2N] on Ni(111) can be derived from the IL-derived C 1s, N 1s, and F 1s spectra (not shown in Fig. 2) taken at 80° emission angle; S 2p and O 1s spectra at 80° were not measured in order to minimize beam damage in the ultrathin layers (see text); also, more bulk-sensitive spectra of the IL-derived peaks at 0° were not measured. As outlined in the text, changes in orientation from a bilayer (sandwich) arrangement to a checkerboard arrangement occur within the first layer, which go along with changes of the relative intensities of the anion- and cation-derived peaks (Figures 3 & 4). In order to average out these effects, we have plotted the sum of the C 1s signals and the sum of the N 1s signals in Figure S1b as a function of deposition time, along with the (solely) anion-derived F 1s signal; Figure S1a shows again the data from Figure 1. For perfect two-dimensional growth, the intensities in Figure S1b should increase sectionwise linearly, with the interceptions (intensities at complete successive layers) following equation S1:

$$\frac{I_{d(n)}}{I_{\infty}} = \left[1 - \exp\left(-\frac{d(n)}{\lambda(E_{kin})\cdot\cos\vartheta}\right)\right] \qquad \text{(S1)}$$

I_{∞} is the Ni $2p_{3/2}$ intensity of an infinitely thick IL layer, *d(n)* the total film thickness of *n* completed layers, ϑ the emission angle with respect to the surface normal, and $\lambda(E_{Kin})$ the inelastic mean free paths of corresponding C 1s, N 1s or F 1s electrons. Up to completion of the first layer, the C1s and N1s data agree with the red straight line in Figure S1, which was obtained using an averaged IMFP for the C1s and N1s electrons of 2.6 nm. This behaviour is in very good agreement with the proposed two-dimensional growth of the first layer. The F1s data lie slightly above the blue straight line, obtained using the corresponding IMFP of 1.9 nm. While this difference is just above the error bars, it qualitatively fits due to the enrichment of the CF_3 groups at the outer surface (see Scheme 2).

For coverages above 1 ML, the experimental C 1s, N 1s and F 1s data in Figure S1b lie below the corresponding straight lines, indicative of a deviation from perfect two-dimensional growth at these coverages. This observation is in line with the conclusion drawn from the damping of the Ni 2p3/2 signal in Figures 1 and S2a (see text).

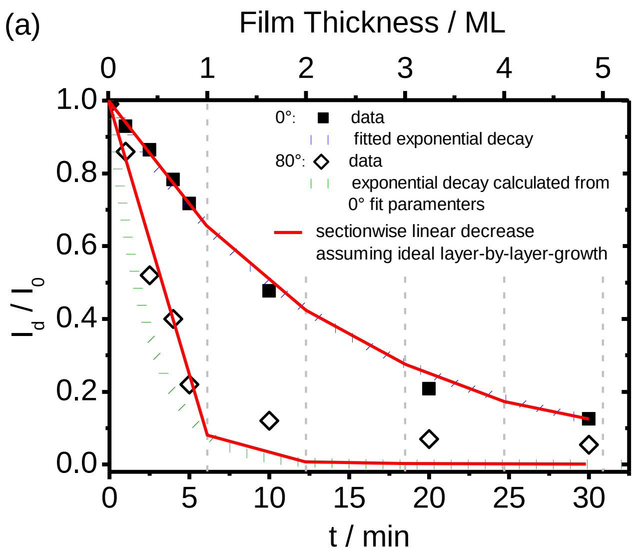

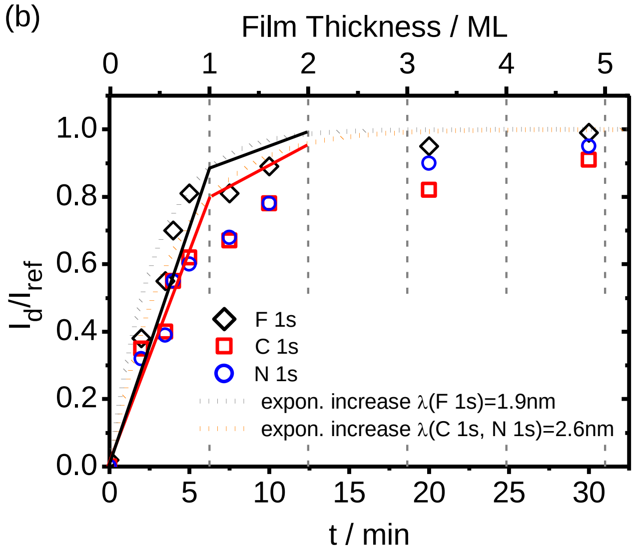

Fig. S1:

(a) Decay of the Ni $2p_{3/2}$ substrate signal as a function of deposition time and, thus, of the amount of IL deposited, for emission angles of 0° (solid squares) and 80° (open diamonds) with respect to the surface normal. The dotted blue line represents an exponential fit to the 0° data according to Equation (2), while the dotted green curve is calculated from the 0° fit parameters taking the additional factor cos 80° into account. An ideal two-dimensional layer-by-layer growth should follow along the red straight sections.

(b) Increase of IL signal intensities (anion F 1s: diamonds, sum of cation and anion C 1s: squares, sum of cation and anion N 1s: circles) measured in 80° as function of deposition time and amount of IL deposited. The dotted lines follow an exponential increase according to Equ. (S1) taking different IMFP values into account. An ideal two-dimensional layer-by-layer growth should follow along the red (for C 1s and N 1s) and black (for F 1s) straight sections. (for details, see text).